ROYAL SOCIETY
OF CHEMISTRY

COMMUNICATION

Solid phase synthesis of functionalised SAM-forming alkanethiol–oligoethyleneglycols†

James Murray,[ab] Dominika Nowak,[bc] Laurynas Pukenas,[bd] Rizuan Azhar,[e] Mathieu Guillorit,[a] Christoph Wälti,[c] Kevin Critchley,[bd] Steven Johnson[e] and Robin S. Bon*[ab]

We present an efficient solid phase synthesis methodology that provides easy access to a range of functionalised long-chain alkanethiol–oligoethyleneglycols that form well-defined self-assembled monolayers on gold and are compatible with pre- or post-assembly conjugation of (bio)molecules. We demonstrate the versatility of our synthetic route by synthesising LCAT–OEGs with a range of functional moieties, including peptides, electro-active redox groups, chemical handles for post-assembly conjugation of (bio)molecules, and demonstrate the application of our LCAT–OEG monolayers in immunosensing, where they show good biocompatibility with minimal biofouling.

Self-assembled monolayers (SAMs) of functionalised long-chain alkanethiolates (LCATs) on metals[1] provide an excellent and versatile platform for the chemoselective immobilisation of (bio)molecules on planar and nanoparticle surfaces. Their well-defined thickness, structure, and dielectric properties[2] make them ideally suited for applications where a high degree of control of the physical and chemical properties of surfaces is required. Functionalised LCATs also enable the creation of patterned surfaces[3] critical for protein and DNA microarrays. SAMs used for protein biosensing applications usually require LCATs incorporating oligoethylene glycol (OEG) linkers to help reduce non-specific protein adsorption[4] and functional groups that allow the further tuning of surface chemistry providing control over the immobilisation, density and orientation of capture molecules. Thus, easy access to a variety of functionalised LCAT–OEGs is essential for optimisation of, for example, immobilisation chemistry and OEG and alkanethiolate length.

However, commercial availability of functionalised LCAT–OEGs is severely limited and synthetic routes often laborious. In this study, we present a versatile solid phase synthesis route that provides easy access to a range of functionalised LCAT–OEGs. Using a range of surface characterisation techniques including surface plasmon resonance (SPR) and electrochemical spectroscopy, we demonstrate that the resulting LCAT–OEGs form dense, well-defined mixed SAMs of high quality, which are compatible with on-surface bioorthogonal ligation reactions.

Customised SAMs presenting ligands and/or biomolecules can be prepared according to two general strategies (Fig. 1): (i) conjugation of (bio)molecules to LCAT–OEGs after SAM formation (*post-assembly conjugation*); (ii) total synthesis of functionalised LCAT–OEGs followed by SAM formation (*pre-assembly conjugation*). Post-assembly conjugation requires robust, chemoselective, and mild chemistry to ensure complete surface functionalisation without side reactions.[2,5] For pre-assembly conjugation approaches, total synthesis of LCAT–OEGs terminated with, amongst others, biotin,[6] peptides,[6c,7] ferrocene,[8] azides,[9] aminooxy groups,[9] and sugars[10] has been demonstrated. Such functionalised LCAT–OEGs are usually synthesised in solution, which requires multiple chromatographic steps and suffers from poor overall yields. Solid phase chemistry presents an attractive alternative for synthesising
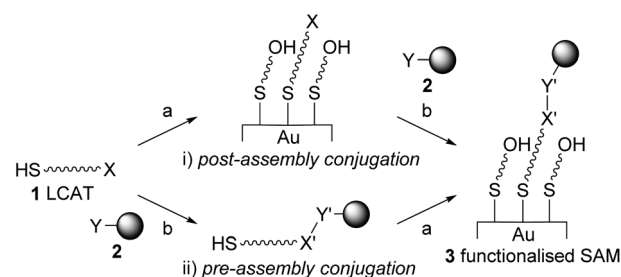
a School of Chemistry, University of Leeds, LS2 9JT, UK. E-mail: r.bon@leeds.ac.uk
b Astbury Centre for Structural Molecular Biology, University of Leeds, UK
c School of Electronic and Electrical Engineering, University of Leeds, UK
d School of Physics and Astronomy, University of Leeds, UK
e Department of Electronics, University of York, Heslington York, YO10 5DD, UK
† Electronic supplementary information (ESI) available: Synthesis and characterisation of compounds, XPS, EIS, AFM, contact angle measurements, CV, colorimetry and SPR. See DOI: 10.1039/c4tb00573b

Fig. 1 SAM functionalisation strategies. (a) SAM formation (in the example: a mixed SAM, with a hydroxy-terminated diluent, on a gold surface); (b) conjugation of LCAT **1** with reagent **2** (in which functional groups X and Y react to form linker X′Y′).

This journal is © The Royal Society of Chemistry 2014

J. Mater. Chem. B, 2014, 2, 3741–3744 | 3741

LCAT–OEGs. The groups of Whitesides and Mrksich have demonstrated the attachment of a thiol-protected LCAT–OEG to resin-bound peptides,[7b,11] while Albericio *et al.* have successfully used 2-chlorotrityl chloride resin to construct biotinylated[6b] and peptide-containing[7a] LCAT–OEGs. However, for applications that require a quick, iterative fine-tuning of SAM properties/functionalities, currently available syntheses are often not sufficient. To address this need, we developed a flexible solid phase synthesis that gives access to a range of LCAT–OEGs through late-stage functionalisation, while minimising intermediate purification.

OEGs are often linked to LCATs through an ether bond. However, in analogy to Albericio's approach,[6b,7a] we chose to use an amide linker, which has been shown to improve SAM stability through the formation of networks of hydrogen bonds.[12] We first synthesised amino-OEGs **6** through the silver(I) oxide-mediated mono-tosylation of oligoethyleneglycols **4** (ref. 13) followed by tosyl displacement with sodium azide and Staudinger reduction (Scheme 1A).[14] Next, **6a**, **6b** and **7** were

coupled to 2-chlorotrityl resin-bound 11-mercaptoundecanoic acid (11-MUA) **9** (Scheme 1B). The terminal alcohol of **10c** was tosylated and treated with sodium azide to afford resin-bound azide **12**. Reduction of **12** under Staudinger conditions proved sluggish, but proceeded rapidly with tin thiophenolate[15] to afford resin-bound amine **14**.

Using Fmoc-solid phase peptide synthesis, we demonstrated that **14** is an excellent starting point for the synthesis of LCAT–OEG–peptide conjugates such as **17** (for pre-assembly functionalisation strategies) or LCAT–OEG **18** incorporating the redox probe methylene blue (MB; Scheme 1C). MB was chosen for electrochemical analysis of SAMs (see below) because of its superior aqueous stability compared to ferrocene.[16] MB-functionalised LCAT–OEG **18** was synthesised by acylating resin-bound amine **14** with carboxylate **16**, which was prepared by adapting a procedure described by Pheeney *et al.* (Scheme S1.1†).[17] Reactions were allowed to run until all resin-bound starting material was consumed, according to LC-MS analysis after micro-cleavage. The immobilised molecules can be
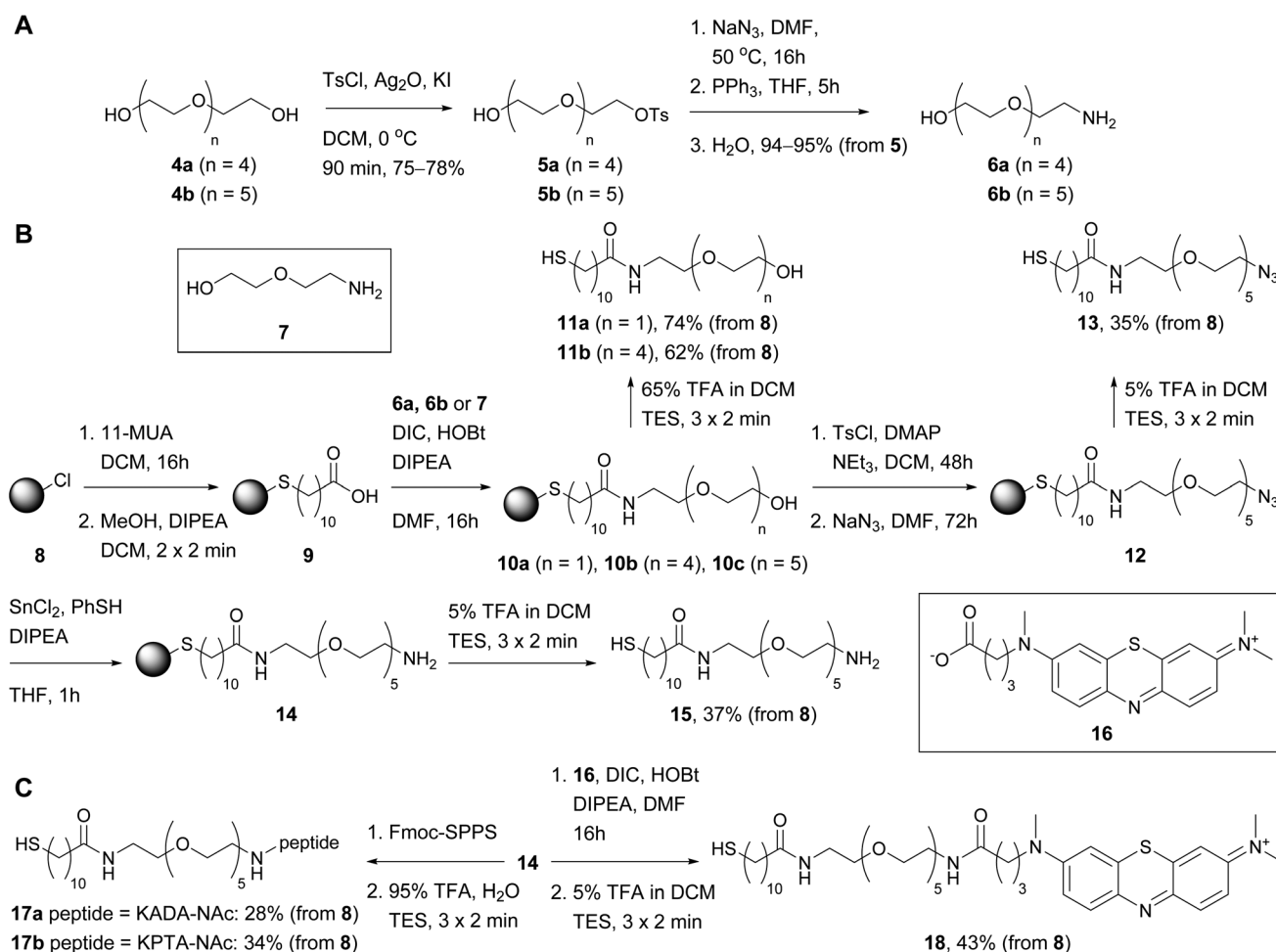
Scheme 1 Synthesis of LCAT–OEGs: (A) preparation of amino-OEGs **6a** and **6b**. (B) Solid phase synthesis of functionalised LCAT–OEGs on 2-chlorotrityl chloride resin **8**. (C) On-resin synthesis of peptide-labelled LCAT–OEGs **17** and methylene blue-labelled LCAT–OEG **18**. Yields of **11a**, **11b**, **13**, **15**, and **16–18** were calculated after chromatography. Insets: Structures of 2-(2-aminoethoxy)ethanol **7** and methylene blue derivative **16**. Abbreviations: Ac = acetyl; DCM = dichloromethane; DIC = diisopropylcarbodiimide; DIPEA = *N*,*N*-diisopropylethylamine; DMAP = 4-dimethylaminopyridine; DMF = *N*,*N*-dimethylformamide; Fmoc = 9-fluorenylmethyloxycarbonyl; HOBt = 1-hydroxybenzotriazole; 11-MUA = 11-mercaptoundecanic acid; SPPS = solid phase peptide synthesis; TES = triethylsilane; TFA = trifluoroacetic acid; Ts = 4-toluenesulfonyl.

3742 | *J. Mater. Chem. B*, 2014, **2**, 3741–3744

This journal is © The Royal Society of Chemistry 2014

cleaved from the solid support at any point using trifluoroacetic acid and triethylsilane (at least one equivalent to scavenge resin-bound trityl cations). After purification by chromatography (either SiO$_2$ or C18), the pure LCAT–OEGs **11a**, **11b**, **13**, **15**, **17** and **18** were obtained in good total yields, based on the loading of 2-chlorotrityl chloride resin **8**.‡

Next, we analysed the quality of SAMs assembled from our functionalised LCAT–OEGs on sputtered gold surfaces. Using X-ray photoelectron spectroscopy (XPS), we found S 2p peaks of SAMs of **11a**, **11b**, and **13** to have binding energies consistent with the formation of thiolate bonds (Fig. S2.1†). The C 1s region consisted of three peaks for all SAMs, corresponding to the alkyl chain, the OEG chain, and carbonyls (Fig. 2A). The analysis of the N 1s region for SAMs of **13** was complicated due to rapid degradation of the azide group under XPS conditions (see the ESI†). The azide-terminated SAM **13** resulted in a surface that was of slightly lower surface energy than SAMs of **11a** or **11b**. This enabled the degree of mixing in the SAMs between diluents **11a** or **11b** and azide **13** to be estimated by contact angle analysis by applying the Cassie equation[18] (Fig. 2B). The insulating properties of SAMs containing different ratios of **11a** : **15** or **11a** : **17a** were assessed by electrochemical impedance spectroscopy (Fig. S3.1 and S3.2†) The minimum phase angles of −88° to −83° for SAMs of **11a** : **15** and −88° to −87° for SAMs of **11a** : **17a**, measured at 0.1 Hz, correspond to the formation of well-packed, insulating monolayers that are almost free of pinholes and collapsed sites effects. Furthermore, atomic force microscopy

(AFM) of a SAM of **11a** : **17a** (1 : 1) revealed uniform surfaces absent of macroscopic islands resulting from phase separation (Fig. S5.1†). Cyclic voltammetry (CV) measurements of mixed SAMs formed from different ratios of **11b** : **15** (Fig. S6.1–S6.3†) revealed SAM capacitance values of 4.4×10^{-6} F cm^{-1}, which corresponds well with the capacitance of simple LCAT monolayers.[19] Furthermore, the absence of redox peaks due to electron transfer to solution phase redox probe confirms the absence of pin holes within the LCAT–OEG monolayers.

To demonstrate the potential suitability of MB-functionalised LCAT–OEGs for molecular electronics applications, we assessed the redox behaviour of surface-bound MB by CV. CV measurements on SAMs of **18** showed clear oxidation and reduction peaks associated with the MB moiety around −130 mV vs. Ag/AgCl (Fig. 2C). No redox peaks were observed in equivalent CV measurements performed on non-redox active LCAT–OEG SAMs (compounds **15** and **17a**, Fig. S6.1–S6.3†). The peaks are reasonably symmetric with only a small peak separation (9 mV at a scan rate of 200 mV s^{-1}), typical of the electrochemical behaviour of a fully reversible redox-active monolayer. Furthermore, the peak anodic and cathodic current was found to increase linearly with scan rate (see inset of Fig. 2C), again characteristic of a surface-tethered redox-active group. From the gradient of the straight line fit to peak current vs. scan rate we calculated a surface coverage, $\Gamma = 8.8 \times 10^{13}$ molecules per cm^2. This is slightly lower than the theoretical density predicted for a perfect SAM formed from LCATs only (4×10^{14} molecules per cm^2) and is likely due to the steric hindrance of the bulky OEG and MB groups that inhibit denser monolayer assembly. Finally, the FWHM of the oxidation and reduction peaks was found to be 37 mV (at 200 mV s^{-1}). While this is lower than the theoretical ideal (45.3 mV for a 2 electron process) we note that deviations in the FWHM are not uncommon in densely packed redox-active monolayers due to electrostatic interactions between adjacent charged species.

Confident that our molecules formed well-defined SAMs, we demonstrated that they also allow (bio)molecule immobilisation by common post-assembly conjugation techniques: Copper-catalysed azide-alkyne cycloaddition (CuAAC) and bis-(sulfosuccinimidyl) suberate (BS3)-mediated amide coupling.

First, we 'clicked' propargyl biotin onto a SAM of **11a** : **13** (1 : 1; see ESI†) and tested for the presence of biotin attached covalently to the surface using a colorimetric assay (Fig. 3A). Briefly, we introduced streptavidin-alkaline phosphatase fusion protein to the surface and used western blue as a stain. Only spots where biotin had been successfully linked to the surface were stained purple (Fig. 3A, S7.1 and S7.2†). Finally, we tested the suitability of SAMs containing amine **15** for immobilisation of the clinically relevant human chorionic gonadotropin antibody (anti-hCG).[20] A SAM of **11a** : **15** (1 : 1) was formed and activated using the bis-succinimide crosslinker BS3 on a Biacore SPR chip (Scheme S8.1†). Injection of anti-hCG gave a much stronger signal in the channel pre-treated with BS3 than in the control channel (no BS3), indicating successful covalent immobilisation of anti-hCG (Fig. 3B). The lack of binding observed on the control channel suggests the LCAT–OEG monolayer is efficient at minimising non-specific adsorption.
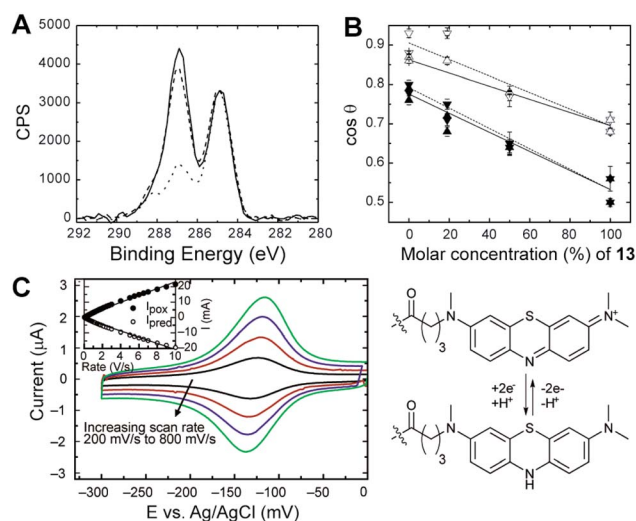

Fig. 2 Characterisation of LCAT–OEG SAMs. (A) XPS data of C 1s region for reference SAMs of **11a** (dotted), **11b** (dashed) and **13** (solid) normalised to the alkyl chain peak at 284.9 eV. Spectra reflect similar carbonyl (288.3 eV), but varying amount of OEG (286.9 eV) carbon. (B) A linear change in cosine of the contact angle with molar ratio of azide **13** in mixed SAMs was observed. Triangles facing down represent **11a** : **13**; facing up – **11b** : **13** SAMs; advancing and receding angles are filled and open symbols, respectively. Dotted and solid lines represent the line of best fit for the Cassie equation for contact angles for **11a** : **13** and **11b** : **13** SAMs, respectively. (C) Typical cyclic voltammograms (left) for the 2-electron oxidation/reduction of SAM-bound methylene blue (right) at scan rates of 200 (black), 400 (red), 600 (blue) and 800 mV s^{-1} (green). The inset shows the linear relationships between current and scan rate.

This journal is © The Royal Society of Chemistry 2014
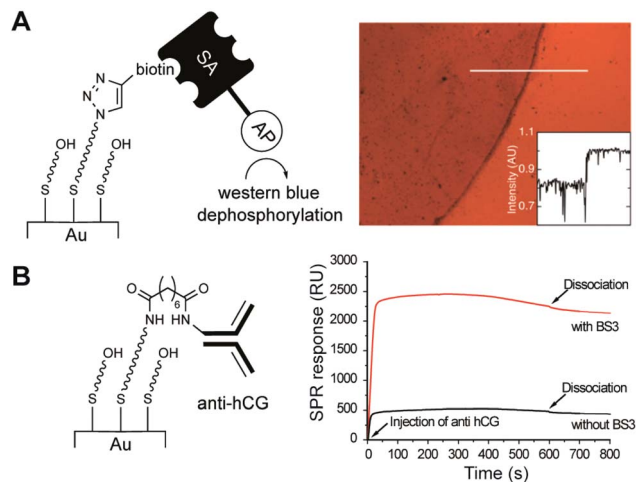
J. Mater. Chem. B, 2014, 2, 3741–3744 | 3743

Fig. 3 Post-assembly conjugation: (A) biotin immobilised through CuAAC on SAMs of **11a** : **13** (1 : 1; left) was detected colorimetrically, as purple spots (right), upon incubation of the gold slide with streptavidin-alkaline phosphatase (SA-AP) and western blue. (B) Immobilisation of anti-hCG on a BS3-activated amine SAM (**11a** : **15**, 1 : 1; left) was detected by SPR (right).

In conclusion, we have established a robust and versatile solid phase synthesis of LCAT–OEGs functionalised with alcohols, azides, amines, peptides, and the redox probe methylene blue, thereby significantly expanding the range of LCAT–OEGs that are easily accessible through solid phase approaches such as those reported by Albericio.[6b,7a] All LCAT–OEGs could be isolated in good yields as pure materials, and were used to form dense and well-defined, high quality mixed SAMs absent of macroscopic island formation (AFM data) and pinholes (EIS and CV data). In addition, the ratios of functionalised LCAT–OEGs and diluents on the surface were directly proportional to the ratios of these molecules in the applied solutions. Finally, we demonstrated that in addition to total synthesis of functional LCAT–OEGs for pre-assembly conjugations, our solid phase methodology also allows the use of bioorthogonal post-assembly conjugation techniques.

Acknowledgements

Notes and references

‡ We routinely perform the synthesis of **11a**, **11b**, **13**, **15**, **17** and **18** on a 0.1–0.6 mmol scale per SPE tube, which provides plenty material for optimisation studies with SAMs. Instead of using chromatography, LCAT–OEGs incorporating basic amines can also be purified by precipitation (as their TFA salts) into mixtures of diethyl ether and hexane.

1 J. C. Love, L. A. Estroff, J. K. Kriebel, R. G. Nuzzo and G. M. Whitesides, *Chem. Rev.*, 2005, **105**, 1103–1169.

2 (*a*) P. Jonkheijm, D. Weinrich, H. Schröder, C. M. Niemeyer and H. Waldmann, *Angew. Chem., Int. Ed.*, 2008, **47**, 9618–9647; (*b*) I. Zaccari, B. G. Catchpole, S. X. Laurenson, A. G. Davies and C. Wälti, *Langmuir*, 2014, **30**, 1321–1326.

3 X. Zhou, F. Boey, F. Huo, L. Huang and H. Zhang, *Small*, 2011, **7**, 2273–2289.

4 K. L. Prime and G. M. Whitesides, *Science*, 1991, **252**, 1164–1167.

5 (*a*) J. Li, P. S. Thiara and M. Mrksich, *Langmuir*, 2007, **23**, 11826–11835; (*b*) D. Samanta and A. Sarkar, *Chem. Soc. Rev.*, 2011, **40**, 2567–2592; (*c*) N. Laurent, R. Haddoub, J. Voglmeir, S. C. C. Wong, S. J. Gaskell and S. L. Flitsch, *ChemBioChem*, 2008, **9**, 2592–2596.

6 (*a*) C. Booth, R. J. Bushby, Y. Cheng, S. D. Evans, Q. Liu and H. Zhang, *Tetrahedron*, 2001, **57**, 9859–9866; (*b*) E. Prats-Alfonso, F. García-Martín, N. Bayo, L. J. Cruz, M. Pla-Roca, J. Samitier, A. Errachid and F. Albericio, *Tetrahedron*, 2006, **62**, 6876–6881; (*c*) R. Derda, D. J. Wherritt and L. L. Kiessling, *Langmuir*, 2007, **23**, 11164–11167.

7 (*a*) E. Prats-Alfonso, S. Oberhansl, A. Lagunas, E. Martínez, J. Samitier and F. Albericio, *Eur. J. Org. Chem.*, 2013, **7**, 1233–1239; (*b*) B. T. Houseman and M. Mrksich, *J. Org. Chem.*, 1998, **63**, 7552–7555.

8 P. A. Bertin, M. J. Ahrens, K. Bhavsar, D. Georganopoulou, M. Wunder, G. F. Blackburn and T. J. Meade, *Org. Lett.*, 2010, **12**, 3372–3375.

9 Z. P. Tolstyka, W. Richardson, E. Bat, C. J. Stevens, D. P. Parra, J. K. Dozier, M. D. Distefano, B. Dunn and H. D. Maynard, *ChemBioChem*, 2013, **14**, 2464.

10 M. Kleinert, N. Röckendorf and T. K. Lindhorst, *Eur. J. Org. Chem.*, 2004, **18**, 3931–3940.

11 D. Ryan, B. A. Parviz, V. Linder, V. Semetey, S. K. Sia, J. Su, M. Mrksich and G. M. Whitesides, *Langmuir*, 2004, **20**, 9080–9088.

12 (*a*) S.-W. Tam-Chang, H. A. Biebuyck, G. M. Whitesides, N. Jeon and R. G. Nuzzo, *Langmuir*, 1995, **11**, 4371–4382; (*b*) S. Svedhem, S. C. T. Svensson and B. Liedberg, *Langmuir*, 1999, **15**, 3390–3394.

13 A. Bouzide and G. Sauve, *Org. Lett.*, 2002, **4**, 8781–8783.

14 S. Svedhem, C. A. Hollander, J. Shi, P. Konradsson, B. Liedberg and S. C. Svensson, *J. Org. Chem.*, 2001, **66**, 4494–4503.

15 M. Bartra, P. Romea, F. Urpi and J. Vilarrasa, *Tetrahedron*, 1990, **46**, 587–594.

16 D. Kang, X. Zuo, R. Yang, F. Xia, K. W. Plaxco and R. J. White, *Anal. Chem.*, 2009, **81**, 9109–9113.

17 C. G. Pheeney and J. K. Barton, *Langmuir*, 2012, **28**, 7063–7070.

18 A. B. D. Cassie and S. Baxter, *Trans. Faraday Soc.*, 1944, **40**, 546–551.

19 M. S. Góes, H. Rahman, J. Ryall, J. J. Davis and P. R. Bueno, *Langmuir*, 2012, **28**, 9689–9699.

20 L. A. Cole, *Clin. Chem.*, 1997, **43**, 2233–2243.

3744 | *J. Mater. Chem. B*, 2014, **2**, 3741–3744

This journal is © The Royal Society of Chemistry 2014